Article

Not peer-reviewed version

Chikungunya and Mayaro Viruses Induce Chronic Skeletal Muscle Atrophy Triggered by Pro-inflammatory and Oxidative Response

Mariana Oliveira Lopes da Silva , Camila Menezes Figueiredo , Rômulo Leão da Silva Neris , Iris Paula Guimarães-Andrade , Daniel Gavino-Leopoldino , Leonardo Linhares Miler-da-Silva , Helber da Maia Valença , Leandro Ladislau , Caroline Victorino Felix de Lima , Fernanda Meireles Coccarelli , Claudia Farias Benjamim , Iranaia Miranda *

Posted Date: 21 June 2024

doi: 10.20944/preprints202406.1490.v1

Keywords: Arthritogenic alphavirus; skeletal muscle; chronic atrophy; inflammation and oxidative stress

Article

Chikungunya and Mayaro Viruses Induce Chronic Skeletal Muscle Atrophy Triggered by Pro-Inflammatory and Oxidative Response

Short Title: CHIKV and MAYV Induce Chronic Muscular Atrophy

Mariana Oliveira Lopes da Silva [1,¶], Camila Menezes Figueiredo [1,¶], Rômulo Leão da Silva Neris [1], Iris Paula Guimarães-Andrade [1], Daniel Gavino-Leopoldino [1], Leonardo Linhares Miler-da-Silva [1], Helber da Maia Valença [2], Leandro Ladislau [2], Caroline Victorino Felix de Lima [3], Fernanda Guimarães Meireles Ferreira [3], Claudia Benjamim [4] and Iranaia Assunção-Miranda [1,*]

[1] Department of Virology, Instituto de Microbiologia Paulo de Góes, Universidade Federal do Rio de Janeiro (UFRJ); Rio de Janeiro, Brasil;
[2] Instituto de Ciências Biomédicas, Universidade Federal do Rio de Janeiro (UFRJ), Rio de Janeiro, Brasil;
[3] Instituto D'Or de Pesquisa e Ensino and National Center for Structural Biology and Bioimaging (CENABio), Universidade Federal do Rio de Janeiro (UFRJ), Rio de Janeiro, Brasil.
[4] Instituto de Biofísica Carlos Chagas Filho, Universidade Federal do Rio de Janeiro (UFRJ), Rio de Janeiro, Brasil;
* Correspondence: iranaiamiranda@micro.ufrj.br
¶ These authors contributed equally to this work .

Abstract: Chikungunya (CHIKV) and Mayaro (MAYV) viruses are arthritogenic alphaviruses that promote an incapacitating and long-lasting inflammatory muscle-articular disease. Despite studies pointing out the importance of skeletal muscle (SkM) in viral pathogenesis, the long-term consequences on its physiology after acute injury and the mechanism of persistence of symptoms are still poorly understood. Combining molecular, morphological, Nuclear Magnetic Resonance Imaging, and histological analysis, we conduct a temporal investigation of CHIKV and MAYV replication in a wild-type mice model, focusing on the impact on SkM composition, structure, and repair in the acute and late phases of infection. We found that viral replication and induced-inflammation promote fast loss of muscle mass and reduction of fibers cross sectional area, by inducing muscle-specific E3 ubiquitin ligases MuRF1 and Atrogin expression, that trigger protein breakdown, resulting in acute SkM fibers atrophy. After temporal reduction of inflammation and clearance of infectious viral particles, SkM atrophy persists until the late phase of infection. The genomic CHIKV and MAYV RNAs were still detected in SkM at the late phase, along with increased levels of chemokines and anti-inflammatory cytokines expression. In agreement with the involvement of inflammatory mediators on induced atrophy, neutralization of TNF and the reduction of oxidative stress using monomethyl fumarate, an agonist of *Nrf2*, decreases atrogens expression and atrophic fibers, while increasing weight gain in treated mice. Taken together, these data indicate that arthritogenic alphavirus infection could chronically impact body SkM composition and also harm repair machinery, contributing to a better understanding of mechanisms of arthritogenic alphaviruses pathogenesis and with description of potentially new targets of therapeutic intervention.

Author Summary: Chikungunya (CHIKV) and Mayaro (MAYV) viruses are both mosquito-borne pathogens that cause chronic joint and muscular pain. Skeletal muscle (SkM) is largely abundant and distributed in tissues throughout the body. High frequency, intensity and persistence of muscular symptoms in CHIKV and MAYV patients have been associated with SkM fibers destruction by viral replication and inflammation. However, long-term consequences of acute injury

 doi:10.20944/preprints202406.1490.v1

for muscle physiology still underexplored. Investigating early and late consequences of replication on SkM structure and repair in mice, we demonstrated that CHIKV and MAYV induced-inflammatory environments promote fast muscle protein degradation, reducing muscle mass and fibers calibers, resulting in persistent SkM atrophy. Despite temporal resolution of lesions, the SkM body composition is still chronically reduced, indicating a deficient SkM repair after injury, that could compromise its physiology. Interestingly, we showed that using compounds that reduce inflammation or induce an antioxidant response, decreases SkM atrophy induced by CHIKV and MAYV infection. These are the first evidence that CHIKV and MAYV infection persistently affects SkM recomposition. It expands the current comprehension of mechanisms of lesion and the persistence of symptoms induced by these viruses. Therefore, this can ultimately contribute to the development of new therapeutic strategies.

Keywords: arthritogenic alphavirus; skeletal muscle; chronic atrophy; inflammation and oxidative stress

Introduction

Chikungunya (CHIKV) and Mayaro (MAYV) viruses are arthritogenic alphaviruses from the *Togaviridae* family [1]. Both infections are associated with a febrile disease, similar to other arboviruses, distinguished by the induction of intense and disabling muscle and joint pain [2–6]. The prevalence of muscular symptoms in CHIKV and MAYV infected subjects occurs at high frequency, reaching about 97% and 77% in some reports, respectively [4,7,8]. In addition, patients could develop a chronic phase of disease, where muscular and articular pain persist for months or even years after onset of symptoms [9–12]. It is well established that the long-lasting pain correlates with the maintenance of local inflammatory lesions and increased levels of circulating inflammatory mediators, despite the resolution of viremia [10,12,13]. However, the mechanism of persistent immune activation and the consequences of chronic inflammation on skeletal muscle physiology are still not elucidated.

Skeletal muscle (SkM) precursor cells and also mature fibers are important targets of arthritogenic alphavirus replication [13,14]. Muscular infection recruits macrophages and also T lymphocytes, which occurs in association with bone destruction [15–18]. Interestingly, the pathogenicity of different epidemic CHIKV strains was positively correlated with the amplitude of replication in the SkM tissue [8,19,20]. Moreover, analysis of muscle biopsies from CHIKV patients with chronic myalgia and also from experimental models of infection suggests that muscle tissue is a site of persistence of viral antigens, including genomic RNA, which may contribute to chronic immune activation [13,15,17,21,22]. Consistent with these findings, mice infection with an engineered CHIKV strain exhibiting restricted replication in SkM, despite comparable replication in other target tissues, results in decreased disease development, including reduction on footpad swelling and intraosseous inflammation [23]. This experimental evidence shows the crucial role of muscle replication and induced inflammation in the progression of arthritogenic alphavirus-induced disease.

Chronic inflammation has been assigned with the promotion of long-term consequences for SkM structure and physiology [24,25]. Cytokines secreted by muscular and immune cells are key regulators of SkM myogenesis, metabolism and reparative programs control after lesions, however, they also drive to myopathies and functional loss in acute and chronic disease [25]. Previously we and other research groups characterized the involvement of the innate and adaptive immune response to the restriction of MAYV and CHIKV replication [26–28]. Type I interferon signaling and cellular adaptive immune response were essential to restrict replication and promote tissue clearance of CHIKV and MAYV [26–30]. However, they have also been associated with dysregulated muscle proteostasis and muscle mass restoration in other clinical conditions [24]. This highlights the complex virus-muscular cell interactions associated with replication and long-term symptoms that have not been addressed.

 doi:10.20944/preprints202406.1490.v1

Here we performed a temporal investigation of MAYV and CHIKV replication in a wide-type mice model, focusing on early and late impact on SkM fibers structure, composition, and repair after injury. We found a positive correlation of MAYV and CHIKV replication with the destruction of muscle fiber, fast loss of muscle mass, and inflammatory response, that results in chronic muscle atrophy. Furthermore, we showed that muscle mass waste and atrophy could be prevented by blocking TNF and inducing an antioxidant response. Together, our data provide the firsts evidence that MAYV and CHIKV induced-inflammation promotes muscle protein degradation and also harms SkM repair machinery, resulting in long-term deficit in body SkM composition and maintenance of lesions that could compromise its physiology.

Material and Methods

Virus Propagation

Mayaro virus (ATCC VR 66, strain TR 4675) and Chikungunya virus (BHI3745/H804709, kindly provided by Dr. Amilcar Tanuri) were propagated at BHK-21 (ATCC-CCL-10) and in C6/36 cells, respectively, using a multiplicity of infection (MOI) of 0.01. After 30 hours of infection culture medium from each infection was collected and centrifuged at 2000 g for 10 minutes to remove cellular *debris* and stored in aliquots at −80 °C. Viral titer of the stock was determined by plaque assay.

Mice Infection and Treatment

Wild-type about 12-day-old SV129 mice of 5.8-6.5 g were subcutaneously infected with 10^5 or 10^6 pfu of MAYV or CHIKV in the left footpad, using a final volume of 20 µL. The same volume of virus-free cell cultured medium (Mock) was used as the control. Each experimental group was housed individually in polypropylene cages with free access to chow and water. Young mice were housed with the uninfected mother during all the experiments. For TNF blockade, mice were treated with Infliximab (IFX - Remicade; Janssen-Cilag/Switzerland) daily via intraperitoneal (i.p.) inoculation of 20 µg or the same volume of vehicle (PBS - 137 mM NaCl, 10 mM sodium phosphate, 2.7 mM KCl, pH 7.4) after infection. Treatment with mono-Methyl fumarate (MMF - Sigma-Aldrich) was carried out 4 hours before Mock or virus infection, by i.p. inoculation of 20 mg/kg or vehicle (same % of DMSO) via i.p. and one dose daily in the following days. Experimental groups were monitored for clinical signals, weight gain, and paw edema (left), which was measured using a digital caliper. Tissue samples were collected at desired days post infection and stored at -80°C until processed or fixed in 4% formaldehyde for future analysis.

Ethics Statement

All experimental procedures performed were in accordance with protocol and standards established by the National Council for Control of Animal Experimentation (CONCEA, Brazil) and approved by the Institutional Animal Care and Use Committee (CEUA), from Universidade Federal do Rio de Janeiro (protocol n° A04/22-036-18, CEUA-UFRJ, Rio de Janeiro, Brazil).

Virus Quantification

MAYV and CHIKV titers in tissue samples and cell cultures were determined by plaque assay in Vero cells. Samples were homogenized in DMEM using a fixed relation of mass/volume (w/v) and after serial dilution of 10-fold, were used to infect confluent Vero cells seeded in 24-well plates. After 1 h of adsorption, the medium was removed and 2 mL of 1% carboxymethylcellulose (w/v) (Sigma-Aldrich) in DMEM with 2% fetal bovine serum (FBS, Invitrogen) were added and cells were incubated at 37°C. After 48 h, cells were fixed using 4% formaldehyde and plaques were then visualized by staining with 1% crystal violet in 20% ethanol. The title was calculated as plaque forming units per mL (pfu/mL) and converted to pfu/g of tissue.

 doi:10.20944/preprints202406.1490.v1

Muscle Structural Analysis

For hind limb SkM weight, mice tendon to tendon gastrocnemius muscle was carefully dissected and immediately weighed. For histological analysis, gastrocnemius was collected at defined days post-infection and fixed with 4% of formaldehyde for 24 h. Tissues were embedded in paraffin after dehydration. Paraffin-embedded tissue sections of 5 mm were prepared and stained with hematoxylin and eosin (H&E). Images were obtained using optical microscopy with a magnification of 10 X (Olympus BX40) and analyzed using ImageJ software for quantifications of muscle fibers cross sectional area (CSA). Briefly, the area of individual fibers of SkM cross sections were calculated after determinations of image pixel/μm converting scale using microscope image scale. The average fiber CSA of a field was taken from at least 4 animals per condition.

Nuclear Magnetic Resonance Imaging (NMRI)

Muscle volume from hind limb along with viral infection was accompanied and NMRI was performed in collaboration with the National Center for Structures and Bioimaging (CENABIO-UFRJ). Images of skeletal muscle cross sections of Mock and MAYV infected mice were acquired using a 7.0 Tesla MRI system (Varian 7T scanner, 210 mm horizontal bore, Agilent Technologies, Palo Alto, CA, USA). The areas of section were combined to muscle volume reconstitution (mm^3) along with the time for each mouse. The same procedure was used for bone analysis.

Gene Expression and Viral RNA Quantification

Hind limb gastrocnemius muscles were homogenized in DMEM using a fixed relation of 0.2 mg of tissue/μL, and 200 μL of the homogenate was used for RNA extraction with Trizol (Invitrogen) according to the manufacturer's instructions. Purity and integrity of RNA were determined by the 260/280 and 260/230 nm absorbance ratios. One microgram of isolated RNA was submitted to DNAse treatment (Ambion, Thermo Fisher Scientific Inc) and then reverse-transcribed using the High-Capacity cDNA Reverse Transcription Kit (Thermo Fisher Scientific Inc). Quantification of cytokines expression was performed using a real-time PCR analysis using Power SYBR kit (Applied Biosystems; Foster City, CA, United States). Cycle threshold (Ct) values were normalized to a housekeeping gene and analyzed using the $^{\Delta\Delta}$Ct method to generate fold change values ($2^{-\Delta\Delta Ct}$). For the detection of genomic RNA of CHIKV and MAYV real-time PCR analysis was conducted using TaqMan Mix kit with specific dyes (ThermoFisher Scientific Inc). A standard curve using viral stocks was constructed to determine CT of the limit of genomic RNA positive samples. Primer and TaqMan dyes sequences are described in Table 1.

Table 1. Primers and TaqMan dyes sequences.

Gene	Fw (5′-3′)	Rv (5′-3′)
CHIKV	AAA GGG CAA ACT CAG CTT CAC	GCC TGG GCT CAT CGT TAT TC
CHIKV - FAM	/56-FAM/ CGC TGT GAT ACA GTG GTT TCG TGT G/ 3BHQ_1	
MAYV	CCT TCA CAC AGA TCA GAC	GCC TGG AAG TAC AAA GAA
MAYVV - FAM	/56-FAM/ CAT AGA CAT CCT GAT AGA CTG CCA CC/ 3BHQ_1	
Atrogin	AGA AAA GCG GCA CCT TCG	CTT GGC TGC AAC ATC GTA GTT
MuRF1	GAG AAC CTG GAG AAG CAG CTC AT	CCG CGG TTG GTC CAG TAG
TNF-α	CCT CAC ACT CAG ATC ATC TTC TCA	TGC TTG TCT TTG AGA TCC ATG C
IFN-γ	AGC AAC AGC AAG GCG AAA A	CTG GAC CTG TGG GTT GTT GA
IL-6	TCA TAT CTT CAA CCA AGA GGTA	CAG TGA GGA ATG TCC ACA AAC
IL-1β	GTA ATG AAA GAC GGC ACA CC	ATT AGA AAC AGT CCA GCC CA
KC	CAC CTC AAG AAC ATC CAG AGC	AGG TGC CAT GAG AGC AGT CT
MCP-1	GTC CCC AGC TCA AGG AGT AT	CCT ACT TCT TCT CTG GGT TG
RANTES	GTG CCC ACG TCA AGG AGT AT	CCT ACT TCT TCT CTG GGT TG
TGF-β	GAC CGC AAC AAC GCC ATC TA	AGC CCT GTA TTC CGT CTC CTT

 doi:10.20944/preprints202406.1490.v1

IL-10	TAA GGG TTA CTT GGG TTG CCA AG	CAA ATG CTC CTT GAT TTC TGG GC
Gapdh	AGG TCG GTC TGA ACG GAT TTG	TGT AGA CCA TGT AGT TGA GGT CA
β-actina	GAC GTT GAC ATC CGT AAA	GTA CTT GCG CTC AGG AGG AG

Quantification of Reactive Oxygen Species.

Left hind limb gastrocnemius of mock and infected mice were dissected at 4 dpi and gently homogenized in cold DMEM (Invitrogen; 1:10 w/v) using a glass tissue grinder as previously described [31]. Reactive oxygen species (ROS) was determined using 2μM of 5-(and-6)-chloromethyl-2',7'-dichlorodihydrofluorescein diacetate acetyl ester (CM-H2DCFDA - Invitrogen) at a 1:1 mixture of homogenate/DMEM. DCF fluorescence was measured at the time of addition and after 30 minutes of incubation in the dark at 37°C in a fluorescence microplate reader (VICTOR™ X3 – PerkinElmer), at 492-495/517-527 nm, as recommended by manufacturers. The absolute values of basal fluorescence of each sample were discounted from that obtained at the end of the DCF incubation and plotted as fold change from the media of Mock values.

Statistical Analysis

We used for comparisons between MAYV and CHIKV groups multiple t test and statistical significance was determined using the Holm-Sidak method. Comparison involving Mock group we used one-way or two-way ANOVA followed by Tukey's multiple comparison test, as indicated. All tests performed using Graph Pad Prism version 6.00 for Windows, Graph Pad Software, La Jolla, CA, United States.

Results

MAYV and CHIKV Replication Induce Skeletal Muscle Fiber Atrophy

CHIKV and MAYV long-term immune activation and consequences in muscle composition and physiology have been underexplored. Thus, we first conducted a temporal investigation of CHIKV and MAYV replication and clearance at SkM after subcutaneous infection at the left footpad in young wild-type mice model (Figure 1). After inoculation, both viruses replicate and increase 4 logs of infectious viral loads just 1-day post-infection (dpi) at hind limb gastrocnemius, being sustained at similar levels until 4 dpi to CHIKV and 6 dpi to MAYV infection (Figure 1A). MAYV and CHIKV were also detected at high infectious loads in the left quadriceps and paw at 4 dpi, but were also detected in other organs such as liver, spleen, and brain (Figure 1B). Despite similar levels in the majority of tissue at this time-post infection, the CHIKV load at the right quadriceps was significantly lower (Figure 1B,C) and was cleared from SkM and other non-articular tissues at 8 dpi (Figure 1C). The MAYV is still being detected in SkM and also for both viruses at the right and left paw, however with decreasing loads (Figure 1C). Despite similar replication and viral persistence in mice paw, CHIKV induced-edema was higher and longer sustained than observed in MAYV infection (Figure 1D), indicating that it does not correlate with the amplitude of viral load. The reduction of weight gain was one of the earliest and most striking clinical signs induced by CHIKV and MAYV infection, and it seems to positively correlate with the amplitude of the peak of viral replication at 4dpi (Figure 1E). Dissecting and weighing the gastrocnemius muscle at this time-point we observed a significant reduction of size and weight, evidencing that MAYV and CHIKV infections induce fast skeletal muscle mass waste (Figure 1F).

Structural SkM analysis at 4 dpi showed an inflammatory process in gastrocnemius muscle, with cellular infiltrate close to the focus of fiber disorganization, and necrosis, mainly in CHIKV infected muscle (Figure 2A). We also evidenced areas with reduced fiber calibers, characteristic of induced muscle atrophy, including leukocyte infiltrate and necrotic areas. Quantification of SkM fiber cross sectional area (CSA) from images confirmed that MAYV and CHIKV significantly reduced the fiber area after infection (Figure 2B). To characterize the global impact of infection on the muscle mass volume, sections of SkM from the hind limb were analyzed by nuclear magnetic resonance imaging (NMRI) and reconstituted to determine volume (Figure 2C). Comparison between Mock and MAYV

 doi:10.20944/preprints202406.1490.v1

infected representative NMRI section of SkM before and at day 4 after infection (D4) showed that while Mock mice present a robust growth of muscle mass, MAYV induces mass waste and loss of fiber structure (Figure 2C). Reconstitution of muscle volume showed a significant reduction of SkM mass from the hind limb along MAYV infection mainly at 4 dpi (Figure 2D). We did not observe differences in tibia or fibula volumes, (Figure 2E) indicating that bone growth was not affected.

Figure 1

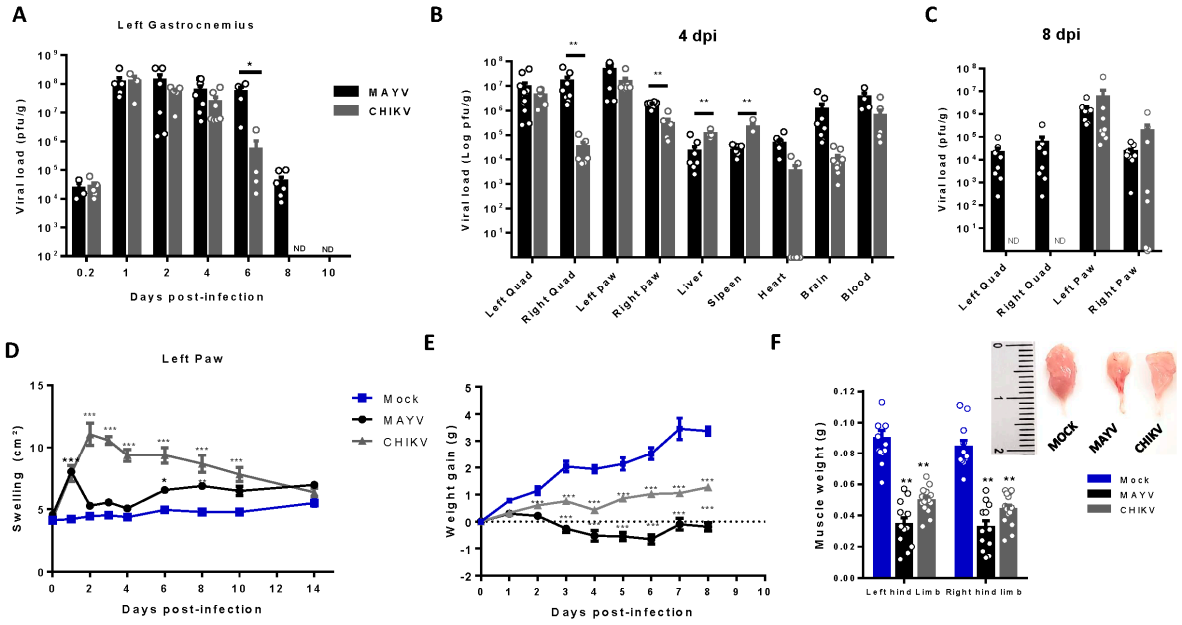

Figure 1. Temporal investigation of CHIKV and MAYV replication and clearance from SkM after subcutaneous infection in young wild-type mice model. Wild-type (WT) SV129 mice of 12 day-olds were subcutaneously infected with MAYV or CHIKV in the left footpad and tissues were collected at indicated time points. (A) Temporal quantification of viral load by plaque assay in the left gastrocnemius, (B) distribution in other tissues with detected infectious at 4 dpi and (C) at 8dpi. (D) Virus- and Mock-infected mice swelling area of left paws and (E) weight gain was accompanied temporally. (F) Gastrocnemius muscle was dissected and immediately weighed at 4 dpi. Values were plotted as mean ± Standard Error of Mean (SEM). The inset shows a representative image of dissected muscles. Statistical analyses were performed for the comparison of (A-C) viral load of MAYV and CHIKV groups by multiple *t test* and significance was determined using the Holm-Sidak method; (D and E) swelling and weight gain curve by two-way ANOVA and (F) muscle weight by one-way ANOVA followed by Tukey's multiple comparison test from MAYV and CHIKV groups with mock. **P < 0.05, **P < 0.01 and *** P< 0.001*. Quad = quadriceps muscle.

To determine the possible mechanism involved in acute SkM mass loss, we evaluated the expression of two muscle-specific E3 ubiquitin ligases that trigger protein breakdown by ubiquitin-proteasome system, muscle atrophy F-box (atrogin-1), and muscle ring finger protein 1 (MuRF1; [32,33]). We found that CHIKV and MAYV infection promoted a significant increase of MuRF1 and atrogin-1 expression in SkM at 4 dpi (Figure 2F). Taken together, this data indicates that MAYV and CHIKV infections promote an unbalance in protein homeostasis by induction of a catabolic process of SkM.

 doi:10.20944/preprints202406.1490.v1

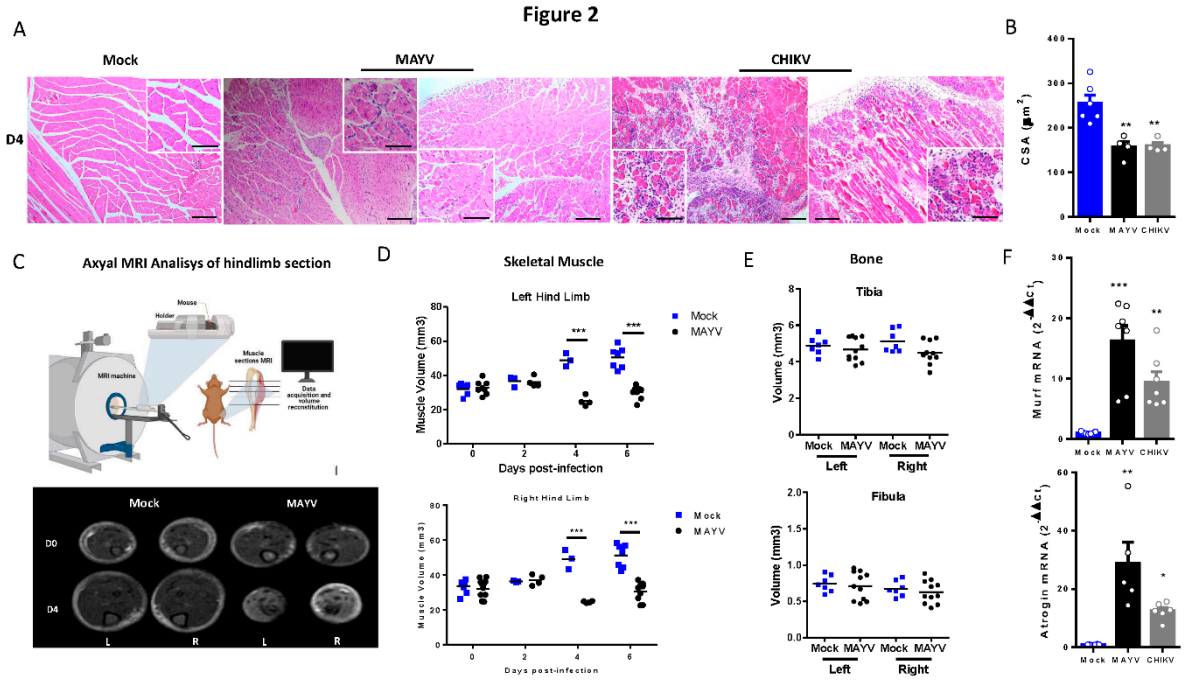

Figure 2. MAYV and CHIKV replication induces inflammatory infiltrate and lesions, muscle mass loss, and fiber atrophy in skeletal muscle. (A) Left gastrocnemius of Mock or infected groups were collected at 4 dpi and stained with hematoxylin and eosin (H&E). Representative images from 2 infected mice demonstrate the inflammatory cell infiltration, fiber destruction, necrosis and atrophic fibers in MAYV- and CHIKV-infected animals. High magnification images inset highlights the atrophic fibers regions. Scale bars of figure=100 μm and inset 50 μm (B) Quantification of SkM fibers cross sectional area (CSA) from H&E stained muscle images was performed using image J software. Each dot corresponds to the average CSA of fibers present in a field per mouse. (C-E) Hind limb of Mock- and MAYV-infected mice was imaged by NMRI. At each time point, images from five sections were acquired and used to calculate the area and were combined to volume reconstitution. (F) Expression levels of MuRF1 and Atrogin in the left gastrocnemius at 4 dpi were determined by real-time PCR analysis. Cycle threshold (Ct) values were normalized to a housekeeping gene and analyzed using the ΔΔCt method to generate fold change values ($2^{-\Delta\Delta Ct}$). Values are shown as mean ± Standard Error of Mean (SEM). Statistical analyses were performed using one-way ANOVA followed by Tukey's multiple comparison test (B and F) and for the comparison of tissue volumes of Mock and MAYV groups multiple *t test* were used and the significance was determined by the Holm-Sidak method. $^{*}P < 0.05$ and $^{**}P < 0.01$. Image C was created with BioRender.com. .

Skeletal Muscle Atrophy and Genomic RNA Persist at Late Phase of Infection

Muscle atrophy persistence could impact muscle development, physiology, and also motor functions, being associated with chronic disease [34]. Late-time analysis of body composition showed that muscle atrophy persists even after infectious viral particles clearance (Figure 3A,B). Together with corporal differences, dissected SkM weight of gastrocnemius was significantly lower at 30 dpi (Figure 3B). Interestingly, despite viral infectious particles that could not be detected after 15 dpi, CHIKV and MAYV genomic RNAs persist at SkM tissue (Figure 3C). Confirming muscle atrophy persistence, structural analysis reveals intense inflammation and atrophic SkM fibers at 8 and 15 dpi (Figure 3D). In addition, fiber CSA was still reduced 15- and 30-days post MAYV and CHIKV infections. Inflammatory infiltrate was also reduced at 30 dpi, but we are still observing fibers with reduced caliber and with centralized nuclei, indicating that CHIKV and MAYV infections trigger chronic SkM atrophy.

 doi:10.20944/preprints202406.1490.v1

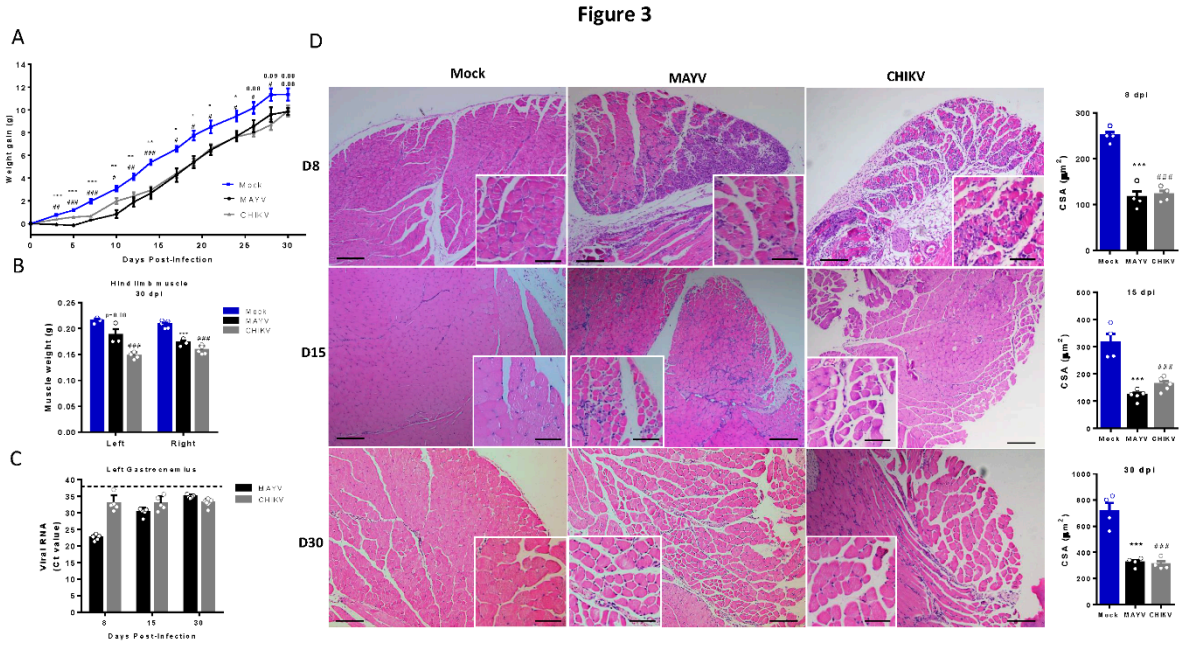

Figure 3. Skeletal muscle atrophy and genomic RNA persist at a late phase of MAYV and CHIKV infection. Wild-type (WT) SV129 mice of 12 day-olds were infected and SkMs were analyzed at late times post infection. (A) Body weight was accompanied until 30 dpi and (B) gastrocnemius muscles were dissected and immediately weighed. (C) CHIKV and MAYV RNA were detected by TaqMan real-time PCR analysis. Dotted lines represent Ct value limit for positive samples. (D) Temporal histological analyses of left gastrocnemius stained with H&E and respective quantification of SkM fiber cross sectional area (CSA) from H&E stained muscle images using image J software. Each dot corresponds to the average CSA of fibers present in a field per mouse. Scale bars of figure=100 μm and inset 50 μm. Values are shown as mean ± Standard Error of Mean (SEM). Statistical analysis of weight gain curve comparing MAYV and CHIKV groups with Mock was performed by two-way ANOVA (A); for muscle weight and CSA, one-way ANOVA was performed (F) followed by Tukey's multiple comparison test. $^{*}P < 0.05$ and $^{**}P < 0.01$. *** *P< 0.001.*

Atrogens Activation Occurs at Early Phase of Infection Associated with Inflammatory Mediators

Inflammatory mediators, such as TNF, IFN-γ, IL-1β, IL-6, and ROS are one of the most important signals that activate ubiquitin-ligases expression that induced SkM catabolism and atrophy [24,35]. We quantify the expression of these cytokines in early (4 and 8 dpi) and late-phase (15 dpi) of CHIKV and MAYV infections and observed a significant increase, mainly of TNF and IFN-γ, but also of IL-6 and IL-1β, however only at early phase (Figure 4A–D). We also investigated the expression of chemokines responsible for the recruitment of inflammatory cells in the infection of arthritogenic alphavirus. Interestingly, while KC/IL-8 and MCP-1 presented higher levels of expression at acute phase (Figure 4E,F), RANTES/CCL5 recruitment signal was increased at 8 dpi and the expression was greater after viral clearance of SkM (Figure 4G). However, the expression of all chemokines analyzed remained significantly increased when compared to the mock at 15 dpi. We also observed a persistent activation of IL-10 and TGF-β expression, mainly at acute (8 dpi) but also at late-phase (15 dpi) of infection (Figure 4H,I). Quantification of ROS production at 4 dpi indicates that MAYV and CHIKV infection induces an oxidant environment at SkM for atrogens expression (Figure 4J). Finally, investigation of MuRF1 and Atrogin expression at 8 and 15 dpi indicates that the signal for activation of persistent atrophy occurs at early phase of infection (8 dpi) but not at 15 dpi, following the acute profile of inflammatory mediators (Figure 4K,L).

Muscle Atrophy Can Be Reduced by Blocking TNF or Inducing Antioxidant Pathways

Despite its long duration, the mechanisms associated with the activation of SkM atrophy seem to be triggered by inflammatory mediators induced in the acute phase of infections. So, we next tested

 doi:10.20944/preprints202406.1490.v1

two pharmacological approaches, first neutralizing TNF-α with infliximab (IFX) and also inducing an antioxidant environment by activation of the nuclear factor erythroid 2-related factor (Nrf2) with monomethyl fumarate (MMF), both approved for clinical use, to control the SkM mass waste induced by arthritogenic alphavirus infection. In agreement with the involvement of TNF in the induced atrophy, we observed that daily treatment with IFX after CHIKV infection reduces muscle mass waste, since it increases body weight gain and SkM weight, together with a reduction of levels of atrogin expression in infected mice (Figure 5A–C). Viral load in SkM at 4dpi was similar in untreated and IFX treated mice, indicating that it did not affect viral replication (Figure 5D), and left paw swelling induced by CHIKV was not modified (Figure 5E).

Figure 4

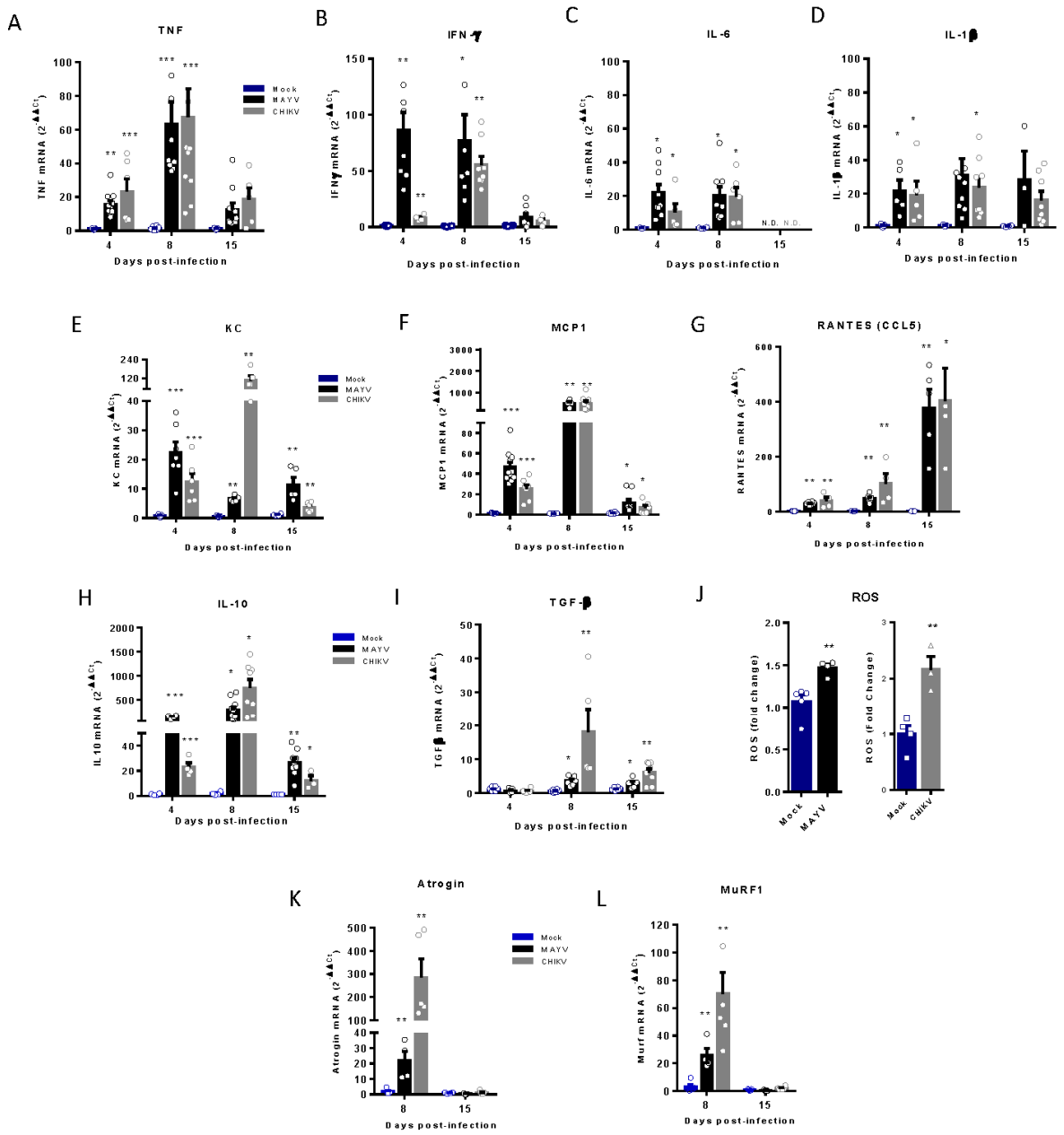

Figure 4. Temporal analysis of inflammatory mediator and atrogens expression at an early and late phase of MAYV and CHIKV infection. Wild-type (WT) SV129 mice of 12 day-olds were

 doi:10.20944/preprints202406.1490.v1

subcutaneously infected with MAYV or CHIKV in the left footpad and left gastrocnemius were collected at indicated time points. (A-I and K-L) Quantification of gene expression using a real-time PCR analysis. Cycle threshold (Ct) values were normalized to a housekeeping gene and analyzed using the ΔΔCt method to generate fold change values ($2^{-\Delta\Delta Ct}$). (J) Total reactive oxygen species (ROS) production in the left gastrocnemius was determined by fluorescence analysis using DCFDA. Arbitrary values of fluorescence from each sample were obtained at the end of the DCF incubation and plotted as fold change from the media of mock values. Values were plotted as mean ± Standard Error of Mean (SEM). Statistical analyses were performed by multiple *t test* comparing Mock with CHIKV and MAYV groups, and the significance was determined using the Holm-Sidak method. **P < 0.05, **P < 0.01, and *** P< 0.001.*

Figure 5

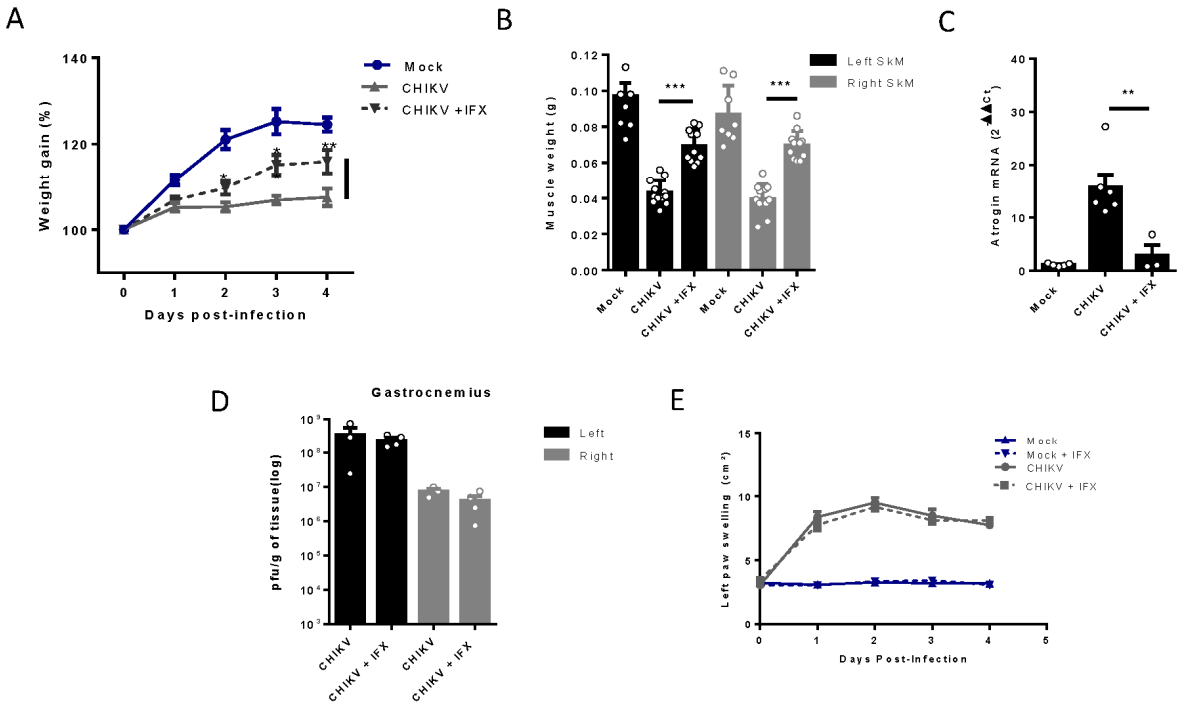

Figure 5. Treatment with Inflixmab reduces muscle mass loss and atrogen expression induced by CHIKV infection. Wild-type (WT) SV129 mice of 12 day-olds were subcutaneously infected with CHIKV and then treated with a daily dose of 20 μg of Infliximab (IFX) or Vehicle (PBS) by i.p. inoculation. (A) Weight gain was accompanied daily and (B) gastrocnemius was dissected at 4 dpi for muscle weight measurement, (C) atrogin expression by real time-PCR, and (D) viral load by plaque assay. (E) Virus- and Mock-infected mice swelling area of left paws was measured daily. Values were plotted as mean ± Standard Error of Mean (SEM). Statistical analyses of weight gain curve and paw swelling comparing treated and untreated CHIKV infected groups were performed by two-way ANOVA (A and E); and for muscle weight, Atrogin expression, and viral load, by one-way ANOVA (F) followed by Tukey's multiple comparison test. **P < 0.05, **P < 0.01 and *** P< 0.001.*

The MMF treatment was initiated 4 hours before CHIKV and MAYV inoculation and also daily in the following days of infection. We observed an improvement in body weight gain since 2 dpi with MMF treatment, a higher SkM weight, and a reduction of levels of atrogens, MURF, and Atrogin, mainly in CHIKV infection (Figure 6A–D). Finally, structural analysis of muscle at 8 dpi reveals preserved muscle fiber structure, together with a global reduction in SkM inflammatory infiltrate (Figure 6E). In addition, we observed reduced areas of atrophic fibers, consistent with an increase in fibers CSA, indicating an efficiency control of SkM atrophy (Figure 6E,F). Interestingly, treatment

 doi:10.20944/preprints202406.1490.v1

with MMF also promoted an improvement in viral load control of CHIKV at 4 dpi and of MAYV at 8 dpi (Figure 6G).

Figure 6

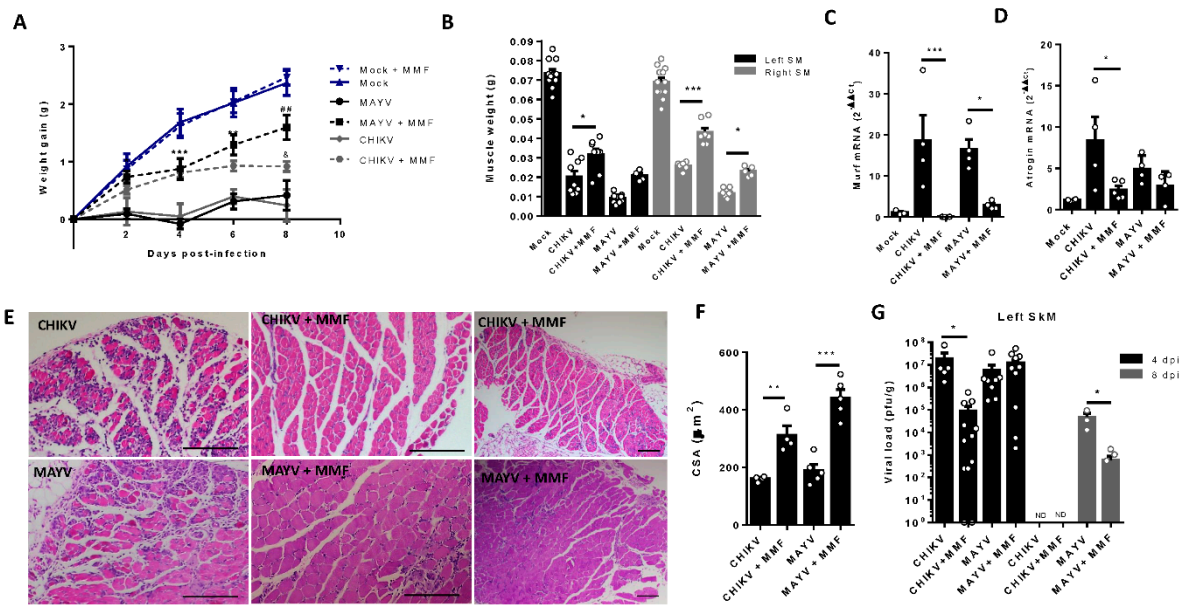

Figure 6. Treatment with MMF reduces muscle atrophy and inflammation induced by MAYV and CHIKV infection. Wild-type (WT) SV129 mice of 12 day-olds were intraperitoneally treated with 20 mg/kg of monomethyl fumarate (MMF) or Vehicle (DMSO) and after 4 h infected with MAYV or CHIKV in the left footpad. (A) Weight gain was accompanied daily. Symbols were used for indicates significance for treatment of both *MAYV and CHIKV group; # Only MAYV and & only CHIKV. Gastrocnemius were dissected at 8 dpi for analysis of (B) muscle weight, (C) MuRF1, and (D) Atrogin expression by real time-PCR. (E) Histological analysis of left gastrocnemius stained with H&E (Scale bars of figures=100 μm) and (F) respective quantification of SkM fiber cross sectional area (CSA) from muscle images using imageJ software. (G) Viral load at SkM was determined by plaque assay at 4 and 8 dpi. Values were plotted as mean ± Standard Error of Mean (SEM). Statistical analyses of weight gain curve comparing treated and untreated CHIKV and MAYV infected groups were performed by two-way ANOVA (A) with; and for muscle weight, Atrogens expression, CSA, and viral load, by one-way ANOVA (B-D, and F-G), followed by Tukey's multiple comparison test. **/& $P < 0.05$, **/## $P < 0.01$ and *** $P < 0.001$.*

Discussion

Arthritogenic alphavirus infections are responsible for a musculoskeletal disease in humans that, despite low lethality, induces persistent debilitating symptoms, even incapacitating to work [2,36,37]. The CHIKV, due to its epidemiological history, global distribution, and current number of cases in tropical regions [38–40], has been one of the most studied members of this group. However, these viruses share similarities and differences in the mechanism of promotion of tissue lesions that need to be individually addressed for better comprehension of their pathogenesis [18,41]. Despite the robust characterization of immune cells and mediators involved in joint disease progression [17,30,42–44], the acute and chronic impact of the inflammatory process on muscle cell physiology was poorly investigated. At present, we conducted a temporal analysis focusing on the SkM inflammatory disease in mice by CHIKV and MAYV infection. We consistently demonstrated that viral replication and inflammatory mediators trigger a fast and intense loss of muscle mass loss, resulting in SkM chronic atrophy (Figure 7). Our data significantly contributes to a better understanding of long-term consequences of arthritogenic alphaviruses to SkM physiology, especially of MAYV infection, a neglected virus from the American continent with increasing and recent expansion into urban areas [45,46].

 doi:10.20944/preprints202406.1490.v1

Figure 7

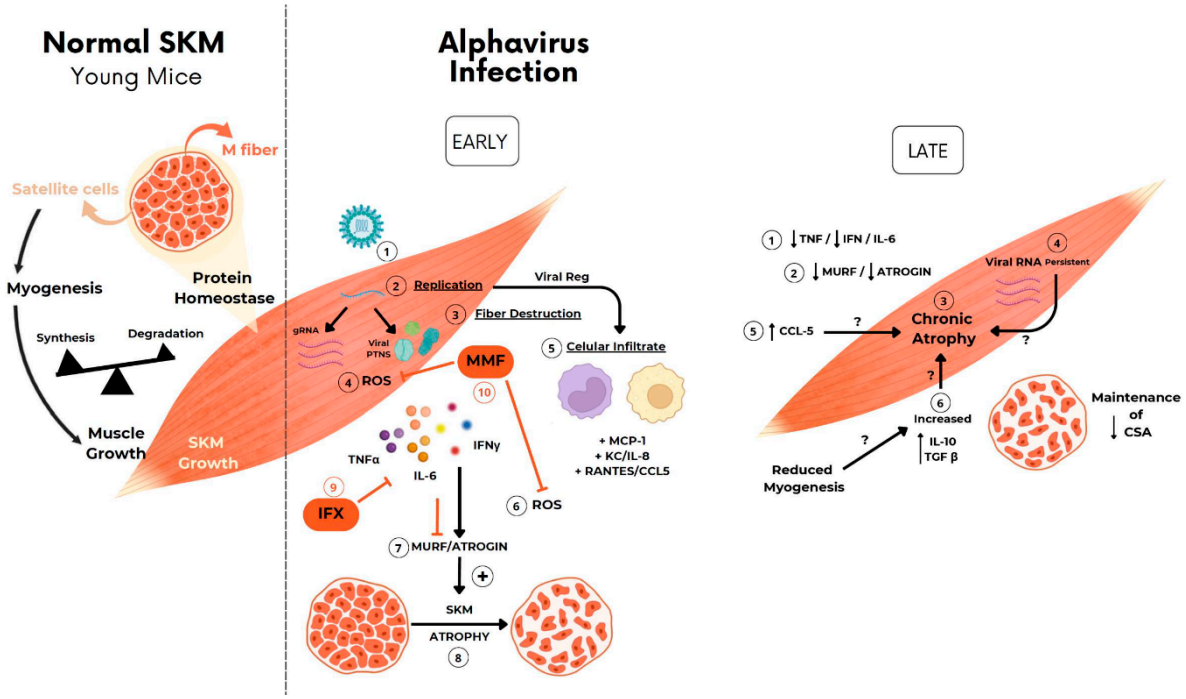

Figure 7. Schematic representation of the possible mechanism involved in arthritogenic alphavirus induced early and late skeletal muscle atrophy. (1) At physiological conditions, young-mice SkM fibers growth along life is determined by individual muscle fiber enlargement and mass gain by a higher rate of synthesis than protein degradation. (2) New fiber generation by myogenesis will be recruited mainly after injury by activation of quiescent satellite cells. (3-8) Arthritogenic alphavirus replicates in SkM fibers resulting in fiber destruction, recruitment of immune cells, production of inflammatory mediators at early phase of infection. (9-10) Induced-inflammation induce protein degradation by UPS by activation of MuRF1 and Atrogin that drives acute SkM atrophy. (11-12) Treatment with IFX or MMF reduces protein degradation and atrophy, corroborating the involvement of these pathways in MAYV- and CHIKV-induced atrophy. (13) SkM atrophy persists at a late phase of infection. (14) Despite the decrease in TNF, IFNγ and IL-6 and also Atrogens expression levels, (15-17) chemokines, IL-10, TGFβ mediators, and viral genomic RNA are still detected, indicating a not complete viral clearance. (18) Long-term immune activation results in the reduction of CSA by a UPS-independent mechanism.

SkM growth in young mice occurs mainly through a process of hypertrophy that drives individual muscle fiber enlargement and mass gain, determined by a higher rate of synthesis than protein degradation [47]. In addition to swelling on infected paws, the reduction of weight gain was one of the earliest clinical signs of CHIKV and MAYV infections, indicating an impact on protein homeostasis. Using different morphological analyses of SkM at 4 dpi we demonstrated that infection promotes a reduction in muscle mass volume by fiber destruction, and also by shrinking, decreasing muscle mass, and reduction of fiber cross sectional area, characteristics of atrophy [25,34,48]. Muscle atrophy is an acute or chronic pathological condition induced by infectious and noninfectious processes, such as aging and cancer, that results in an imbalance of protein synthesis and degradation [25]. In agreement, a study by Ozden in 2007, evaluating quadriceps biopsy of CHIKV patients with myositis, demonstrated evidence that the infection can promote vacuolization and muscle fibers atrophy [13]. The high incidence of muscular symptoms in other arboviruses, although muscular atrophy has not been evaluated, may indicate that it could be a common feature of viral infections [49]. In addition to CHIKV, SARS-CoV infection was the only one in which acute muscle weakness was associated with histological findings of atrophy in patient biopsy [50], reinforcing our hypothesis, and it should be a focus of future studies.

 doi:10.20944/preprints202406.1490.v1

The persistent atrophy induced by CHIKV and MAYV infections demonstrated by our study in mice model could result in weakness, fatigue, and reduction in global mobility [34]. These same symptoms are largely observed in patients who progress to the chronic phase of arthritogenic alphavirus infection, however, the reduced post-infection quality of life has not been directly associated with muscular atrophy [51]. Interestingly, symptoms are usually more intense in elderly patients, who, in addition to having previous rheumatic complications, also present a chronic loss of muscle mass [52,53]. This evidence demonstrates the translation of our data with what has been observed in the clinic of the arthritogenic alphavirus, highlighting the importance of understanding the molecular mechanisms enrolled in the induction and persistence of SkM atrophy.

The destruction of fibers and precursor cells by viral replication could trigger a local inflammatory response that would be determinant to restore the regular physiology or to progress to persistent myopathies [21,23]. Increased muscle protein degradation can be mediated by several mechanisms, including activation of the protein ubiquitin-proteasome system (UPS) and autophagy-lysosome machinery, which may contribute to a rapid muscle mass loss [24,48]. Some studies *in vitro* using cell culture model demonstrated that activation of UPS and autophagy are essential for efficient CHIKV replication [54–56]. In our mouse model, we found that CHIKV and MAYV replications in SkM enhanced the expression of muscle-specific ubiquitin-ligases MuRF1 and Atrogin, which are involved in the promotion of protein degradation by UPS. Curiously, these atrogens were induced only at an early phase of infection but reduced caliber fibers persisted until adult life (Figure 7). The same profile of early upregulation was observed for inflammatory mediators, such as TNF, IFN-γ, IL-6 and ROS, that are well established activators of muscle degradation by the induction of MuRF1 and Atrogin expression [24,25]. Supporting the association of this inflammatory mediator on induced atrophy, the blockade of TNF and also the reduction of oxidative stress by using an agonist of Nrf2 during early infection, decreases atrogens expression and atrophic fibers, while increases weight gain.

The rate of body weight gain in infected mice increases after viral clearance from SkM at 8dpi, indicating a close relation of muscle mass lost with viral replication. Despite temporally increasing CSA, the difference between CHIKV/MAYV and mock infected mice remains stable, indicating that muscle mass composition was not restored over time. The persistence of viral RNA or proteins in SkM, even in the absence of infectious viral particles assembly, have been raised as possibly responsible for chronic immune activation in arthritogenic alphavirus infection [18]. The MAYV and CHIKV RNA levels were reduced from early phase, but were maintained at detectable levels in the SkM at 30 dpi, confirming that SkM could be a reservoir of viral antigens persistence. Antigen persistence could be a way to maintain signals for muscle degradation or reduce muscle repair machinery, but future investigations are necessary to confirm this hypothesis. A previous study conducted by our group demonstrated that MAYV-induced muscle damage seems to be dependent on lymphocytes infiltrates [26]. Increased levels of CCL5 at 15 dpi could result in the persistence of cellular recruitment signals, such as T-lymphocytes, for SkM [57]. However, this increase, together with the increased levels of IL-10 and TGF-β expression, could also be a shift for the activation of muscle repair cascade [58,59].

The absence of increased levels of atrogens in late phases of infection indicates that other pathways could be involved in the persistence of atrophy, and also needs to be elucidated. Myogenesis is the main process responsible for muscle repair and recomposition after injury, controlled by a balanced pro-inflammatory and followed by an anti-inflammatory immune response [59]. It was demonstrated that ZIKV replication in SkM of neonate mice and also in myoblast cells impairs myogenesis [60,61]. Increased levels of TGF-β have been involved in delays of reparative myogenesis [59]. Thus, since myoblast and myotubes are permissive to arthritogenic virus infection [21], it is possible that chronic-induced atrophy could also be triggered by a delay in muscle repair by dysregulation of muscle myogenesis.

Treatment of CHIKV and MAYV infected mice with MMF not only reduced atrophy but also reduced viral replication, indicating that an antioxidant environment does not seem to be favorable for viral replication. The MMF is a primary metabolite of dimethyl fumarate that was approved for

 doi:10.20944/preprints202406.1490.v1

clinical use in multiple sclerosis patients [62]. In addition to other biological functions, MMF stabilizes and activates the Nrf2 transcription factor, inducing the expression of many target genes coding for antioxidant enzymes, such as HO-1, NAD(P)H:quinone oxidoreductase 1 and proteins for glutathione synthesis [63]. Our data showed an efficient reduction in muscle mass loss, with a significant restoration of fiber CSA and reduction of SkM inflammation and lesion at 8dpi. Since treatment also reduced viral replication, the MMF effect could not only be attributed to the impact of reduction on ROS, but it can be a consequence of both. Thus, our data indicate that the use of antioxidants or the induction of this pathway to promote a less oxidative environment in the acute phase of infection may be a therapeutic strategy for reducing viral load, and also the long-term impact of the infection on muscle composition and which should be better explored.

Author Contributions: Conceptualization: IAM, Methodology: MOLS, CMF, RLSN, IPGA, LLMS, HMV, LL CVFL, FGMF, CB, IAM; Investigation: MOLS, CMF, RLSN, IPGA, DGL, LLMS, HMV, LL, CVFL, FGMF, IAM; Supervision: MOLS, CMF, IAM; Writing—original draft: IAM; Writing—review & editing: MOLS, IPGA, CB, IAM

Acknowledgments: We thanks Dr Amilcar Tanuri for provide Chikungunya virus, technical and structural support from National Center for Structural Biology and Bioimaging (CENABio/UFRJ) and the financial support from Fundação de Amparo à Pesquisa do Rio de janeiro (FAPERJ), Conselho Nacional de Desenvolvimento Científico e Tecnológico (CNPq), and Coordenação de Aperfeiçoamento de Pessoal de Nível Superior (CAPES; finance code 001).

Competing Interests: Authors declare that they have no competing interests.

References

1. Suhrbier, A., M.C. Jaffar-Bandjee, and P. Gasque, *Arthritogenic alphaviruses--an overview.* Nat Rev Rheumatol, 2012. **8**(7): p. 420-9.
2. Santiago, F.W., et al., *Long-Term Arthralgia after Mayaro Virus Infection Correlates with Sustained Pro-inflammatory Cytokine Response.* PLoS Negl Trop Dis, 2015. **9**(10): p. e0004104.
3. Poidinger, M., et al., *Genetic stability among temporally and geographically diverse isolates of Barmah Forest virus.* Am J Trop Med Hyg, 1997. **57**(2): p. 230-4.
4. Tesh, R.B., et al., *Mayaro virus disease: an emerging mosquito-borne zoonosis in tropical South America.* Clin Infect Dis, 1999. **28**(1): p. 67-73.
5. Taylor, S.F., P.R. Patel, and T.J. Herold, *Recurrent arthralgias in a patient with previous Mayaro fever infection.* South Med J, 2005. **98**(4): p. 484-5.
6. Ali Ou Alla, S. and B. Combe, *Arthritis after infection with Chikungunya virus.* Best Pract Res Clin Rheumatol, 2011. **25**(3): p. 337-46.
7. Paquet, C., et al., *Chikungunya outbreak in Reunion: epidemiology and surveillance, 2005 to early January 2006.* Euro Surveill, 2006. **11**(2): p. E060202 3.
8. Lohachanakul, J., et al., *Differences in response of primary human myoblasts to infection with recent epidemic strains of Chikungunya virus isolated from patients with and without myalgia.* J Med Virol, 2015. **87**(5): p. 733-9.
9. Borgherini, G., et al., *Outbreak of chikungunya on Reunion Island: early clinical and laboratory features in 157 adult patients.* Clin Infect Dis, 2007. **44**(11): p. 1401-7.
10. Hoarau, J.J., et al., *Persistent chronic inflammation and infection by Chikungunya arthritogenic alphavirus in spite of a robust host immune response.* J Immunol, 2010. **184**(10): p. 5914-27.
11. Halsey, E.S., et al., *Mayaro virus infection, Amazon Basin region, Peru, 2010-2013.* Emerg Infect Dis, 2013. **19**(11): p. 1839-42.
12. Schilte, C., et al., *Chikungunya virus-associated long-term arthralgia: a 36-month prospective longitudinal study.* PLoS Negl Trop Dis, 2013. **7**(3): p. e2137.
13. Ozden, S., et al., *Human muscle satellite cells as targets of Chikungunya virus infection.* PLoS One, 2007. **2**(6): p. e527.
14. Sane, J., et al., *Prolonged myalgia in Sindbis virus infection: case description and in vitro infection of myotubes and myoblasts.* J Infect Dis, 2012. **206**(3): p. 407-14.
15. Dhanwani, R., et al., *Characterization of chikungunya virus induced host response in a mouse model of viral myositis.* PLoS One, 2014. **9**(3): p. e92813.
16. Chen, W., et al., *Arthritogenic alphaviruses: new insights into arthritis and bone pathology.* Trends Microbiol, 2015. **23**(1): p. 35-43.
17. Morrison, T.E., et al., *A mouse model of chikungunya virus-induced musculoskeletal inflammatory disease: evidence of arthritis, tenosynovitis, myositis, and persistence.* Am J Pathol, 2011. **178**(1): p. 32-40.

 doi:10.20944/preprints202406.1490.v1

18. Kafai, N.M., M.S. Diamond, and J.M. Fox, *Distinct Cellular Tropism and Immune Responses to Alphavirus Infection.* Annu Rev Immunol, 2022. **40**: p. 615-649.
19. Rohatgi, A., et al., *Infection of myofibers contributes to increased pathogenicity during infection with an epidemic strain of chikungunya virus.* J Virol, 2014. **88**(5): p. 2414-25.
20. Hussain, K.M., et al., *Establishment of a Novel Primary Human Skeletal Myoblast Cellular Model for Chikungunya Virus Infection and Pathogenesis.* Sci Rep, 2016. **6**: p. 21406.
21. Young, A.R., et al., *Dermal and muscle fibroblasts and skeletal myofibers survive chikungunya virus infection and harbor persistent RNA.* PLoS Pathog, 2019. **15**(8): p. e1007993.
22. Labadie, K., et al., *Chikungunya disease in nonhuman primates involves long-term viral persistence in macrophages.* J Clin Invest, 2010. **120**(3): p. 894-906.
23. Lentscher, A.J., et al., *Chikungunya virus replication in skeletal muscle cells is required for disease development.* J Clin Invest, 2020. **130**(3): p. 1466-1478.
24. Howard, E.E., et al., *Divergent Roles of Inflammation in Skeletal Muscle Recovery From Injury.* Front Physiol, 2020. **11**: p. 87.
25. Costamagna, D., et al., *Role of Inflammation in Muscle Homeostasis and Myogenesis.* Mediators Inflamm, 2015. **2015**: p. 805172.
26. Figueiredo, C.M., et al., *Mayaro Virus Replication Restriction and Induction of Muscular Inflammation in Mice Are Dependent on Age, Type-I Interferon Response, and Adaptive Immunity.* Front Microbiol, 2019. **10**: p. 2246.
27. Couderc, T., et al., *A mouse model for Chikungunya: young age and inefficient type-I interferon signaling are risk factors for severe disease.* PLoS Pathog, 2008. **4**(2): p. e29.
28. Poo, Y.S., et al., *Multiple immune factors are involved in controlling acute and chronic chikungunya virus infection.* PLoS Negl Trop Dis, 2014. **8**(12): p. e3354.
29. Locke, M.C., et al., *Interferon Alpha, but Not Interferon Beta, Acts Early To Control Chronic Chikungunya Virus Pathogenesis.* J Virol, 2022. **96**(1): p. e0114321.
30. Hawman, D.W., et al., *Chronic joint disease caused by persistent Chikungunya virus infection is controlled by the adaptive immune response.* J Virol, 2013. **87**(24): p. 13878-88.
31. Nem de Oliveira Souza, I., et al., *Acute and chronic neurological consequences of early-life Zika virus infection in mice.* Sci Transl Med, 2018. **10**(444).
32. Bodine, S.C., et al., *Identification of ubiquitin ligases required for skeletal muscle atrophy.* Science, 2001. **294**(5547): p. 1704-8.
33. Gomes, M.D., et al., *Atrogin-1, a muscle-specific F-box protein highly expressed during muscle atrophy.* Proc Natl Acad Sci U S A, 2001. **98**(25): p. 14440-5.
34. Yin, L., et al., *Skeletal muscle atrophy: From mechanisms to treatments.* Pharmacol Res, 2021. **172**: p. 105807.
35. Glass, D.J., *Skeletal muscle hypertrophy and atrophy signaling pathways.* Int J Biochem Cell Biol, 2005. **37**(10): p. 1974-84.
36. Miner, J.J., et al., *Chikungunya viral arthritis in the United States: a mimic of seronegative rheumatoid arthritis.* Arthritis Rheumatol, 2015. **67**(5): p. 1214-1220.
37. Seyler, T., et al., *Estimating the burden of disease and the economic cost attributable to chikungunya, Andhra Pradesh, India, 2005-2006.* Trans R Soc Trop Med Hyg, 2010. **104**(2): p. 133-8.
38. Van Bortel, W., et al., *Chikungunya outbreak in the Caribbean region, December 2013 to March 2014, and the significance for Europe.* Euro Surveill, 2014. **19**(13).
39. Renault, P., et al., *A Major Epidemic of Chikungunya Virus Infection on Réunion Island, France, 2005–2006.* The American Journal of Tropical Medicine and Hygiene Am J Trop Med Hyg, 2007. **77**(4): p. 727-731.
40. *Chikungunya worldwide overview*. 2023 [cited 2023 11/13/2023]; Available from: https://www.ecdc.europa.eu/en/chikungunya-monthly#:~:text=Situation%20update%2C%2023%20August%202023,%2C%20and%20Asia%20(4).
41. Assuncao-Miranda, I., C. Cruz-Oliveira, and A.T. Da Poian, *Molecular mechanisms involved in the pathogenesis of alphavirus-induced arthritis.* Biomed Res Int, 2013. **2013**: p. 973516.
42. Morrison, T.E., et al., *Characterization of Ross River virus tropism and virus-induced inflammation in a mouse model of viral arthritis and myositis.* J Virol, 2006. **80**(2): p. 737-49.
43. Lin, T., et al., *CXCL10 Signaling Contributes to the Pathogenesis of Arthritogenic Alphaviruses.* Viruses, 2020. **12**(11).
44. Haist, K.C., et al., *Inflammatory monocytes mediate control of acute alphavirus infection in mice.* PLoS Pathog, 2017. **13**(12): p. e1006748.
45. Mackay, I.M. and K.E. Arden, *Mayaro virus: a forest virus primed for a trip to the city?* Microbes Infect, 2016. **18**(12): p. 724-734.
46. Caicedo, E.Y., et al., *The epidemiology of Mayaro virus in the Americas: A systematic review and key parameter estimates for outbreak modelling.* PLoS Negl Trop Dis, 2021. **15**(6): p. e0009418.
47. Zammit, P.S., *Function of the myogenic regulatory factors Myf5, MyoD, Myogenin and MRF4 in skeletal muscle, satellite cells and regenerative myogenesis.* Semin Cell Dev Biol, 2017. **72**: p. 19-32.

 doi:10.20944/preprints202406.1490.v1

48. Haberecht-Muller, S., E. Kruger, and J. Fielitz, *Out of Control: The Role of the Ubiquitin Proteasome System in Skeletal Muscle during Inflammation.* Biomolecules, 2021. **11**(9).
49. Filippone, C., et al., *Arboviruses and Muscle Disorders: From Disease to Cell Biology.* Viruses, 2020. **12**(6).
50. Soares, M.N., et al., *Skeletal muscle alterations in patients with acute Covid-19 and post-acute sequelae of Covid-19.* J Cachexia Sarcopenia Muscle, 2022. **13**(1): p. 11-22.
51. Watson, H., et al., *Stiffness, pain, and joint counts in chronic chikungunya disease: relevance to disability and quality of life.* Clin Rheumatol, 2020. **39**(5): p. 1679-1686.
52. Sissoko, D., et al., *Post-epidemic Chikungunya disease on Reunion Island: course of rheumatic manifestations and associated factors over a 15-month period.* PLoS Negl Trop Dis, 2009. **3**(3): p. e389.
53. Jaffar-Bandjee, M.C., et al., *Emergence and clinical insights into the pathology of Chikungunya virus infection.* Expert Rev Anti Infect Ther, 2010. **8**(9): p. 987-96.
54. Karpe, Y.A., K.D. Pingale, and G.D. Kanade, *Activities of proteasome and m-calpain are essential for Chikungunya virus replication.* Virus Genes, 2016. **52**(5): p. 716-21.
55. Thio, C.L., et al., *Differential proteome analysis of chikungunya virus infection on host cells.* PLoS One, 2013. **8**(4): p. e61444.
56. Krejbich-Trotot, P., et al., *Chikungunya triggers an autophagic process which promotes viral replication.* Virol J, 2011. **8**: p. 432.
57. Mageriu, V., et al., *Role of Myokines in Myositis Pathogenesis and Their Potential to be New Therapeutic Targets in Idiopathic Inflammatory Myopathies.* J Immunol Res, 2020. **2020**: p. 9079083.
58. Waldemer-Streyer, R.J., D. Kim, and J. Chen, *Muscle cell-derived cytokines in skeletal muscle regeneration.* FEBS J, 2022. **289**(21): p. 6463-6483.
59. Tu, H. and Y.L. Li, *Inflammation balance in skeletal muscle damage and repair.* Front Immunol, 2023. **14**: p. 1133355.
60. Gavino-Leopoldino, D., et al., *Skeletal Muscle Is an Early Site of Zika Virus Replication and Injury, Which Impairs Myogenesis.* J Virol, 2021. **95**(22): p. e0090421.
61. Legros, V., et al., *Differentiation-dependent susceptibility of human muscle cells to Zika virus infection.* PLoS Negl Trop Dis, 2020. **14**(8): p. e0008282.
62. Berger, A.A., et al., *Monomethyl Fumarate (MMF, Bafiertam) for the Treatment of Relapsing Forms of Multiple Sclerosis (MS).* Neurol Int, 2021. **13**(2): p. 207-223.
63. Yao, Y., et al., *Dimethyl Fumarate and Monomethyl Fumarate Promote Post-Ischemic Recovery in Mice.* Transl Stroke Res, 2016. **7**(6): p. 535-547.